SSIM 2023 – PM Dight (ed.)

doi:10.36487/ACG_repo/2335_08

Probabilistic pit slope stability analysis targeting a reliability-based design acceptance criteria: a parametric study

G Velarde *University of Alberta, Canada*

R Macciotta *University of Alberta, Canada*

Abstract

Design of open pit slopes is a decision-making process which aims to maximise the ore recovery while minimising the excavation volumes. The current practice of designing open pit slopes adopts the widely accepted Guidelines for Open Pit Slope Design by Read & Stacey (2009). An optimum design should satisfy a design acceptance criteria (DAC). However, designing open pit slopes is a complex process that involves inherent risks and uncertainties. As a result, reliability analyses are becoming increasingly important for performance-based slope designs. In a reliability approach, the amount of information on the slope materials and behaviour would reflect the reliability of a slope design. This paper presents a parametric study defined by the uncertainties of the rock mass strength properties and the slope geometric configurations at three different design reliability levels targeting a reliability-based DAC (RBDAC). The reliability assessment is performed using probabilistic analysis adopting the two-dimensional limit equilibrium method and Monte Carlo simulations. The input variables for the rock mass strength are defined through probability density functions (PDF) that capture the natural variability, while the input variables of geological structures are defined through kinematic assessments.

The PDFs of the rock mass strength properties were modelled based on the generalised Hoek–Brown criterion using the mean, coefficient of variation (COV) and dependence between quantitative properties of the criterion. Results show that most of the resultant pairs of Factor of Safety (FoS) and probability of failure and associated COV of the resulting FoS (COV_{FoS}) are consistent with the RBDAC. Based on this, a redesign is proposed showing the applicability of the RBDAC and comparing it to the current DAC. This approach has significant implications for slope optimisation or mitigation plans for future pushbacks in case of instabilities.

Keywords*: reliability-based design acceptance criteria, coefficient of variation, probability density functions*

1 Introduction

Design of open pit slopes is a decision-making process which aims to maximise the ore recovery while minimising the excavation volumes. This decision-making process is subjected to uncertainties related to the geotechnical conditions, ore resources, commodity prices and cost (Darling 2011), which needs to be considered along with acceptable criteria. The widely adopted slope design process and design acceptance criteria (DAC) were published by the Large Open Pit (LOP) project in 2009. The slope design process is an iterative process of analyses performed throughout short- and long-term designs which should target and then meet the DAC. Various approaches have been considered for the slope design, ranging from empirical assessment to advanced numerical assessments.

A typical approach such as deterministic analysis is widely adopted in the industry, and relies on precisely defined values (e.g. average uniaxial compressive strength values) in the calculation of Factor of Safety (FoS). However, it has been recognised that this approach can lead to risky or conservative slope designs. For example, a case study of an open pit diamond mine reported that back-analysis of past failures does not fail at mean values (Martin & Stacey 2018). Based on that experience, subsequent slope stability analyses at this mine were carried out using the 35th percentile values for rock strength (Martin & Stacey 2018). This case study highlights the impact of uncertainty on the slope design process and the decision-making process by

using more conservative values. Consequently, the probabilistic approach is deemed more appropriate as it yields a more robust design, avoiding over-conservatism and risky slope designs.

On the other hand, the 2009 DAC is an FoS–Probability of Failure (PoF) matrix based on different levels of consequences (low, moderate, high) and the scale of the slope (bench, inter-ramp, overall). However, the same FoS does not mean the same for a given degree of uncertainty or level of reliability. In this regard, Macciotta et al. (2020, 2021, 2022) identified that mature operating pits had been transitioning to performance-based designs, allowing operators to adopt lower DAC while ensuring adequate safety levels. Furthermore, it was identified that the target FoS–PoF pairs proposed in the 2009 DAC were inconsistent in terms of the statistical relationship between FoS–PoF. To this end, Macciotta et al. (2020, 2021, 2022) presented a reliability-based DAC (RBDAC) matrix that considers adequate pairs of FoS–PoF that are consistently associated through the coefficient of variation (COV) for different reliability levels and different economic consequences of unsuccessful slope performance. It is noteworthy that the RBDAC considers management of economic risks and not safety risks, because it is assumed that safety risks are kept within tolerable levels and managed through in-house trigger action and response plans.

As an example, Gaida et al. (2021) carried out a thorough evaluation of the components of the slope design process, identifying a high reliability on the geotechnical model. This allowed the design of an alternative targeting a lower FoS, highlighting the benefit-cost reward. Moreover, Creighton et al. (2022) highlighted the significant impact of enhancing reliability in the slope design process on business outcome, by the adoption of a RBDAC and risk-reward approach. This paper presents a parametric study based on the geomechanical characteristics of the rock mass and slope configuration of an open pit mine. The study is performed through probabilistic analysis using the two-dimensional (2D) limit equilibrium method (LEM) along with the Monte Carlo technique. The result of the probabilistic analysis aims to evaluate the uncertainty of the rock mass parameters and the geological structures. The former is assessed through the COV defined by statistical measures. The latter is assessed through stereographic projections, which are further integrated into the stability analysis using a generalised anisotropic strength approach. The integration of geological structures aims to gain insight of the role of epistemic uncertainty in slope stability (in this study, associated with the geometrical configuration of discontinuities and not to the mechanical properties). Calculated values of FoS–PoF pairs and COV are plotted against the 2020 RBDAC. Moreover, to test the applicability of the double-entry matrix, a design of a pushback is developed to provide insights into potential trade-offs between safety, excavation volume and economic benefits.

2 Uncertainty in rock strength

Uncertainty is an important factor in geotechnical engineering because of the inherent randomness and complex heterogeneity of geological settings. Essentially, uncertainty can be categorised as natural (inherent) variability or aleatory uncertainty, and epistemic uncertainty (Baecher & Christian 2003; Hudson & Feng 2015; Kiureghian & Ditlevsen 2008; Ferson & Ginzburg 1996). The former is associated with natural processes, both spatial and temporal (e.g. spatial variability of geological units, occurrence of earthquakes). The latter is associated with a lack of knowledge and understanding, which can be reduced by increasing the data-collection effort. Handling uncertainty is difficult as it cannot be completely eliminated, but an understanding of it is essential in performance-based design and risk-informed decision-making.

Numerous research studies have been undertaken to analyse the natural variability of rock strength. Some studies aimed to assess the natural variability by measuring the COV, which has been linked to various rock types. Hadjigeorgiou and Harrison (2012) found that the COV tends to increase as the degree of anisotropy and heterogeneity in the rock increases. In addition, Bewick et al. (2015) concluded that the natural variability of uniaxial compressive strength (UCS) is higher in heterogeneous rocks compared to homogeneous rocks due to the different failure modes exhibited during laboratory tests. Thus the COV_{UCS} tended to be higher in heterogenous rock datasets than in homogeneous rock datasets. Similarly, Rafiei Renani et al. (2019) investigated the variability of rock strength in high heterogeneous porphyry deposits and reported COV_{UCS} values close to 1, indicating significant variability. On the other hand, the natural variability of the Hoek–Brown parameter, m_i, has not been measured as extensively as the UCS. Phoon & Retief (2016) reported

COV_{mi} values for different types of rocks. Figure 1 depicts a summary of some studies on rock strength variability, illustrating the uncertainty associated with intact rock properties, particularly UCS and m_i.

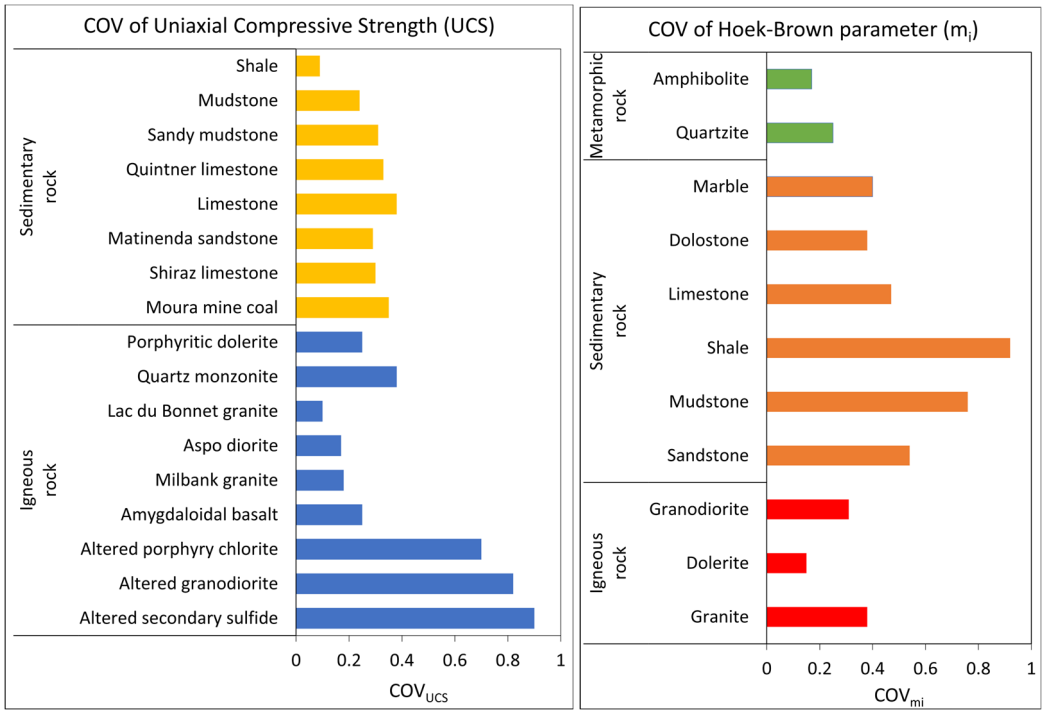

Figure 1 Coefficient of variation of intact rock parameters from a subset of previous studies. (a) Coefficient of variation of Uniaxial Compressive strength; (b) Coefficient of variation of Hoek–Brown parameter (Bewick et al. 2015; Rafiei Renani et al. 2019; Phoon & Retief 2016)

Stochastic models, including probabilistic approaches and Bayesian statistics, have been used to describe and measure quantitatively the random variability in rock strength parameters (Bedi & Harrison 2013). In probabilistic analyses, a probability density function (PDF) is assigned to the random variable, typically characterised by statistical measures such as mean, standard deviation and COV. Common probability distributions used in rock slope engineering include the lognormal and normal distributions. Generally, lognormal distribution can provide an adequate fit, whereas normal distribution can be chosen in the absence of information (Phoon & Retief 2016; Hoek 1998). However, parameters evaluated semi-quantitatively, such as the rock mass rating (RMR) or geological strength index (GSI), may require different PDF representations. The choice of distribution depends on the available information. For instance, Hoek (1998) used a normal distribution to represent the ranges of GSI when analysing the stability of a rock slope with limited information. In this paper, a probabilistic approach was adopted to evaluate uncertainty in rock mass properties (Bedi & Harrison 2013). The disturbance factor (D) referred to the consideration of how mining activities such as blasting, excavation, stress relief and other processes that affect the stability of rock slopes depend on the definition of the damage region. The definition and the extension of the damage zone differs from the assumptions considered from the practitioners and it is difficult to calibrate with real data (Ma et al. 2022). In this regard, the associated uncertainty of the D factor was not assessed in this study.

A specific geological context and the slope geometry of an open pit mining operation is used to develop a comprehensive understanding of parameter uncertainty. In addition, this parametric study is based on available site-specific information and information reported in previous studies.

3 Materials and methodology

This paper is based on a specific geological setting, with the material parameters and slope configurations varying based on their respective levels of engineering effort. These components were adopted from an open

pit mining operation in South America. The open pit mine is a porphyry copper deposit hosted in Late Cretaceous-Paleocene andesite. The andesite is cut by the intrusion of porphyry rocks ranging from quartz monzonite to granodiorite. Figure 2 shows the geological map on the exposed pit (Padilla et al. 2001). Two lithological units are the main rock units exposed in the sector analysed.

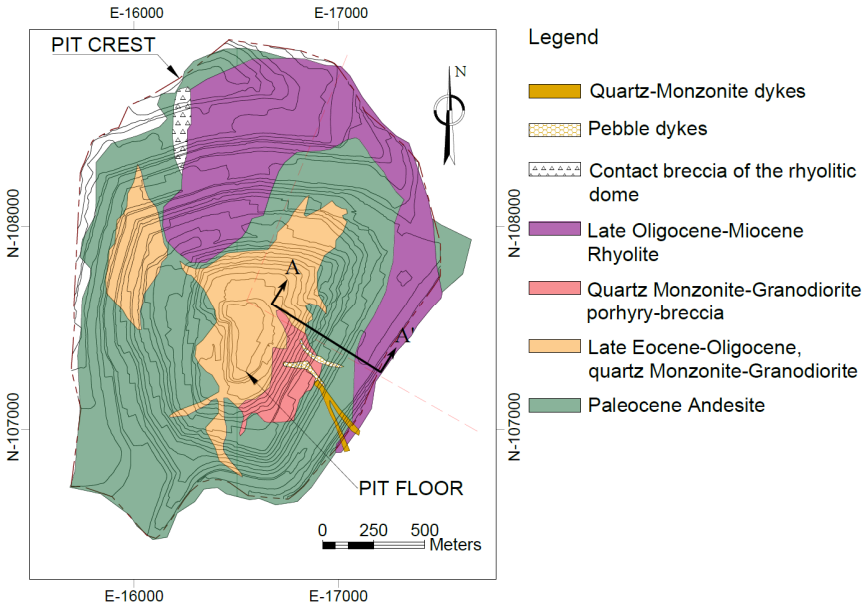

Figure 2 Geological map of the base case used to inform this study (after Padilla et al. 2001)

The geological structures and their interaction with rock mass fabric, leading to medium- to large-scale instabilities (Hustrulid et al. 2001), are integrated into the probabilistic analysis.

Probabilistic slope stability analyses are performed using a 2D LEM adopting the GLE/Morgenstern-Price method. The software used to this end is SLIDE2. Also, the Monte Carlo technique is used to define the input parameters and the associated uncertainty. The workflow adopted is outlined in Figure 3. The workflow begins with the modelling of rock mass strength parameters and their variability in terms of COV, adopting the generalised Hoek–Brown failure criterion. Subsequently, the generalised Hoek–Brown failure parameters were transformed to equivalent Mohr–Coulomb parameters considering the Pearson correlation coefficient. Resultant equivalent Mohr–Coulomb parameters, along with their variability, were then introduced as input parameters to perform stochastic limit equilibrium analysis for evaluation against the 2020 RBDAC. Two types of analyses were carried out (depending on the scenario): one considering rock mass strength failure and one, structurally controlled failure.

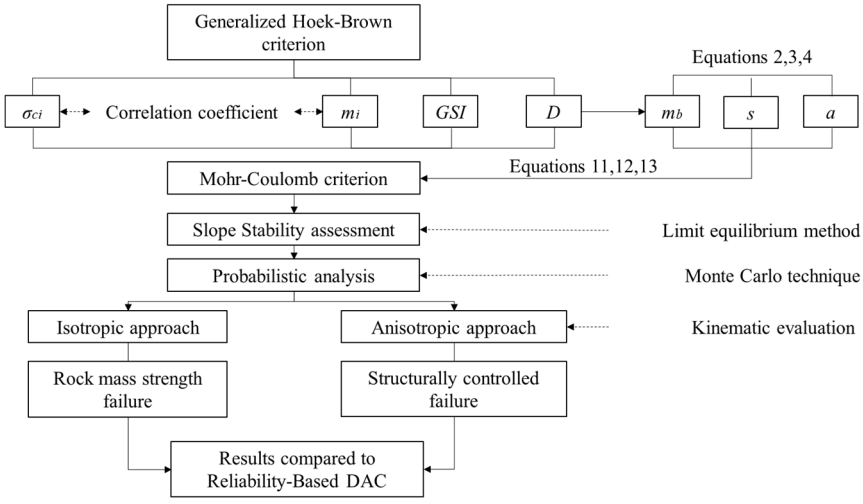

Figure 3 Workflow adopted for probabilistic analyses to test the reliability-based design acceptance criteria

Uncertainty in rock mass strength properties was quantified using stochastic models. These models represent variables generated through defined PDF for σ_{ci}, m_i and GSI were used to randomise rock mass failure envelopes using the generalised Hoek–Brown criterion (Hoek et al. 2002). The Hoek–Brown criterion is expressed by Equations 1 to 4:

$$\sigma_1 = \sigma_3 + \sigma_{ci}\left(m_b \frac{\sigma_3}{\sigma_{ci}} + s\right)^a \tag{1}$$

$$m_b = m_i \exp\left(\frac{\mathrm{GSI} - 100}{28 - 14D}\right) \tag{2}$$

$$s = \exp\left(\frac{GSI - 100}{9 - 3D}\right) \tag{3}$$

$$a = \frac{1}{2} + \frac{1}{6}\left[\exp\left(\frac{-GSI}{15}\right) - \exp\left(\frac{-20}{3}\right)\right] \tag{4}$$

where:

mb, s and a	=	material constants.
GSI	=	geological strength index.
D	=	disturbance factor.

The D factor in this study was set as zero in order to study the undisturbed rock mass behaviour. The dependence between the variables UCS and m_i was calculated through the Pearson correlation coefficient, which was obtained from data collected from published values of five porphyry copper deposits located in the region. To create dependent variables, the method described by Phoon & Ching (2015) was adopted. The method adopted begins with the modelling of two independent standard normal random variables (Z_i, Z_j). Subsequently, the Pearson correlation coefficient is introduced to model two dependent variables (X_i, X_j) according to Equations 5 and 6:

$$X_i = Z_i \tag{5}$$

$$X_j = \delta_{ij} Z_i + \sqrt{1 - {\delta_{ij}}^2} Z_j \tag{6}$$

where δ_{ij} = Pearson correlation coefficient.

Since the dependent variables follow a normal distribution they can be transformed into a different distribution shape, such as lognormal distribution. The transformation from normal to lognormal distribution can be achieved using Equations 7 to 9:

$$Y_i = \exp\left(\lambda_i + \xi_i X_i\right) \tag{7}$$

$$\lambda_i = \ln\left(\frac{\mu}{\sqrt{1 + COV^2}}\right) \tag{8}$$

$$\zeta_i = \sqrt{\ln\left(1 + COV^2\right)} \tag{9}$$

where:

λ_i = mean of ln(Y).

ζ_i = standard deviation of ln(Y).

μ = mean of Y_i.

When adopting generalised Hoek–Brown failure criteria, the input of dependent parameters is often not supported by many commonly used industry software packages. Consequently, each non-linear Hoek–Brown failure envelope was transformed to equivalent linear Mohr–Coulomb criteria. This was done following common practice for pit slope probabilistic analyses. As the conversion to Mohr–Coulomb requires the definition of confining stress limits, these can be defined by the method proposed by Rafiei Renani & Martin (2020). This method evaluates the confining stress using Equation 10:

$$\frac{\sigma_{3,max}}{\gamma H} = \frac{0.175}{\tan(\beta)} \tag{10}$$

where:

H = slope height.

y = unit weight.

β = slope angle.

Hence, the equivalent Mohr–Coulomb parameters were found using the equations suggested by Hoek et al. (2002, 2018) shown in Equations 11 to 13:

$$c = \frac{\sigma_{ci}[(1+2a)s + (1-a)m_b\sigma_{3n}](s + m_b\sigma_{3n})^{a-1}}{(1+a)(2+a)\sqrt{1 + [6am_b(s + m_b\sigma_3)^{a-1}]/[(1+a)(2+a)]}} \tag{11}$$

$$\varphi = \sin^{-1}\left[\frac{6am_b(s + m_b\sigma_{3n})^{a-1}}{2(1+a)(2+a) + 6am_b(s + m_b\sigma_{3n})^{a-1}}\right] \tag{12}$$

$$\sigma_{3n} = \frac{\sigma_{3,max}}{\sigma_{ci}} \tag{13}$$

where:

c = equivalent cohesion.

ϕ = equivalent friction angle.

Kinematic evaluations and statistical analyses on discontinuity information projected onto the stereonet using DIPS v. 8.0 (Rocscience Inc. 2022) were completed to calculate the variability in the orientation of geological structures. This aimed to observe the influence of epistemic uncertainty associated with structural orientation on the distribution of the stochastic calculations of FoS. The shear strength of the geological structures throughout the stability analysis were kept with its deterministic values. Hence the outcomes of the kinematic evaluation were incorporated implicitly and explicitly in the probabilistic slope stability analysis.

Three scenarios were considered and defined based on the level of engineering effort and structure reliability. These scenarios illustrate the enhancement of the reliability level in the open pit slope design. The first scenario represents a pre-mining slope design characterised by limited information. The uncertainty of the intact rock mass parameters was characterised using information from Figure 1. The phreatic level was assumed in the first scenario based on the groundwater conditions chart proposed by Hoek & Bray (1981).

The second scenario represents an implemented phase slope design characterised by improved lithological and structural information. The uncertainty of the intact rock mass parameters is characterised using information obtained from Rapiman & Sepulveda (2006). The third scenario represents an advanced phase slope design that comprises extensive information collected from previous phase-pit excavations and from back-analyses of localised failures. The rock mass strength parameters are characterised through back-analyses criteria, in accordance with the published calibration (Hustrulid et al. 2001).

The results from the scenarios evaluated are plotted against the 2020 RBDAC matrix to illustrate the changes of reliability levels in terms of pairs of FoS–PoF and COV_{FoS} (the coefficient of variation is used as an indicator of design reliability). To validate the shape of the distributions obtained, the goodness of fit is tested using a Q-Q plot and Kolmogorov–Smirnov test. Then the 2020 RBDAC is further utilised to illustrate its application by designing a pushback and compar with a design targeting the 2009 DAC presented by Read & Stacey (2009) in the Guidelines for Open Pit Slope Design. The comparison between the two designs shows the advantages of the 2020 RBDAC over the 2009 DAC in the slope optimisation expressed in terms of the volume excavated.

4 Results and discussion

4.1 First scenario: limited information at the pre-mining phase

A slope design for the pre-mining phase of an open pit mining operation needs an initial assessment, which focuses mainly on defining potential slope configurations. The rock mass properties were chosen from a review of the literature. A generic slope configuration with a slope height of 250 m and an overall slope angle (OSA) of 43° was chosen. The COV of UCS and m_i considered were 0.90 and 0.31, respectively. Likewise, the mean UCS and m_i were 70 MPa and 26 (Read & Stacey 2009; Hustrulid et al. 2001; Phoon & Retief 2016). The rock mass was assumed to be blocky and of fair quality, therefore a range of GSI between 35 and 55 (based on the descriptions reported in literature in Hustrulid et al. 2001) was adopted. A lognormal distribution was assigned to the UCS and m_i, while a uniform distribution was assigned to the GSI. Figure 4 illustrates the relationships between UCS and m_i based on data collected from five porphyry copper deposits in the region. The Pearson correlation coefficient obtained is approximately -0.5.

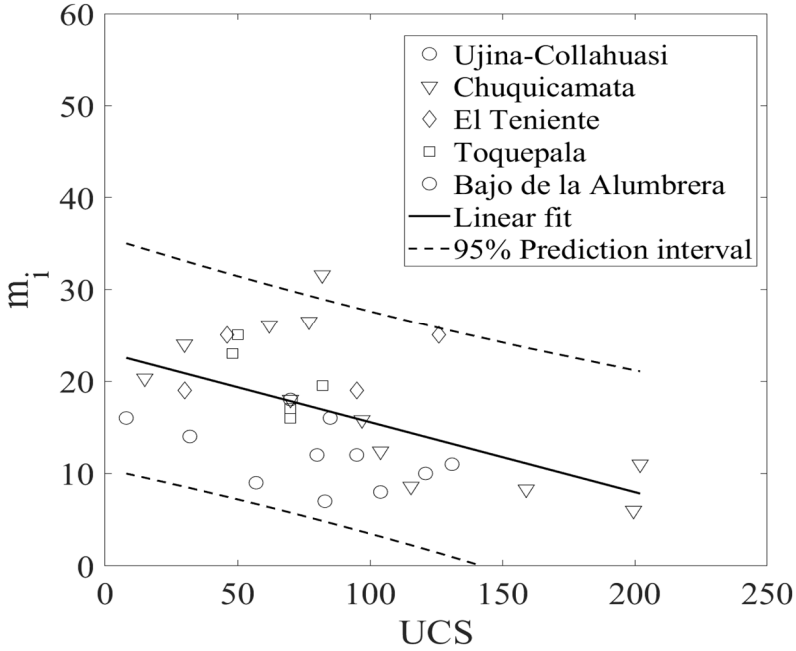

Figure 4 Relationship between uniaxial compressive strength and m_i for the five porphyry copper deposits in the region

Figure 5 shows the process for the modelling of dependent parameters through the Pearson correlation coefficient, statistical measures and assigned adequate PDFs. These dependent parameters, along with the GSI, were used to define the Hoek–Brown envelopes which were subsequently transformed to equivalent Mohr–Coulomb parameters. Given the slope configuration, the confining stress was calculated using Equation 10.

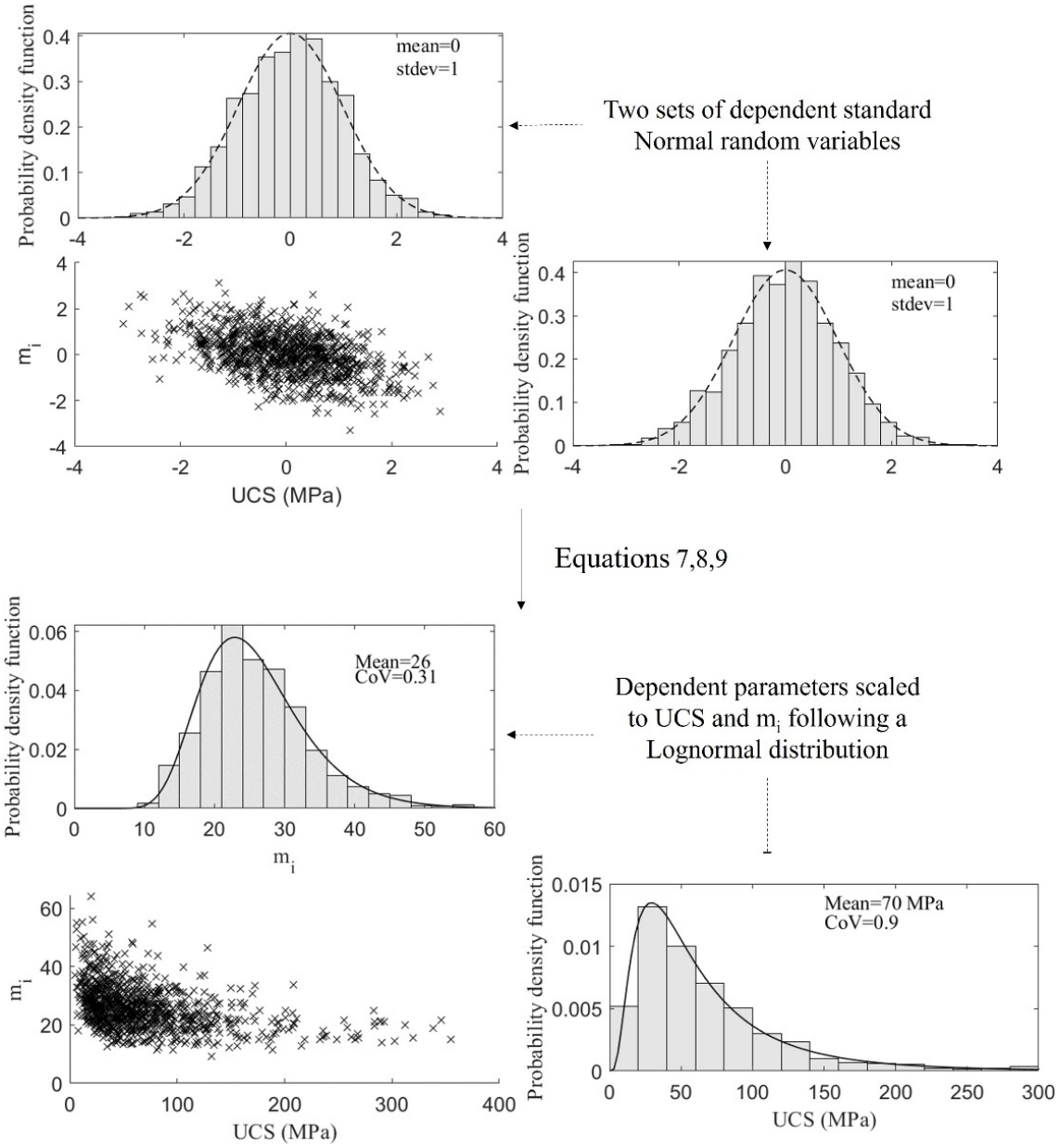

Figure 5 Process for the development of PDFs of dependent parameters (UCS and m_i). The flow illustrates how two sets of correlated normal distributions are built and then scaled to the parameter distributions

Figure 6 illustrates the equivalent cohesion. The goodness of fit was tested through a Q-Q plot as shown in Figure 6c. The results from the Kolmogorov–Smirnov test at the 5% significance level for lognormal distribution (test statistics 0.08 and a p-value 5.0E-06) and for gamma distribution (test statistics 0.11 and a p-value 2.1E-11) indicated a high discrepancy between the observed results and the theoretical distribution. Based on both tests, a lognormal distribution was selected to fit the observed data with a mean of 0.69 MPa and COV of 0.33. Figure 6b illustrates the equivalent friction angle. The goodness of fit was tested through a Q-Q plot as shown in Figure 6d. The results from the Kolmogorov–Smirnov test at the 5% significance level

for normal distribution (test statistics 0.02 and a p-value 0.58) and for lognormal distribution (test statistics 0.04 and a p-value 0.08) indicated a good agreement with the observed results and the theoretical distribution. As the results of the normal distribution were greater than the lognormal distribution, a normal distribution was selected to fit the observed data, with a mean of 56° and COV of 0.09.

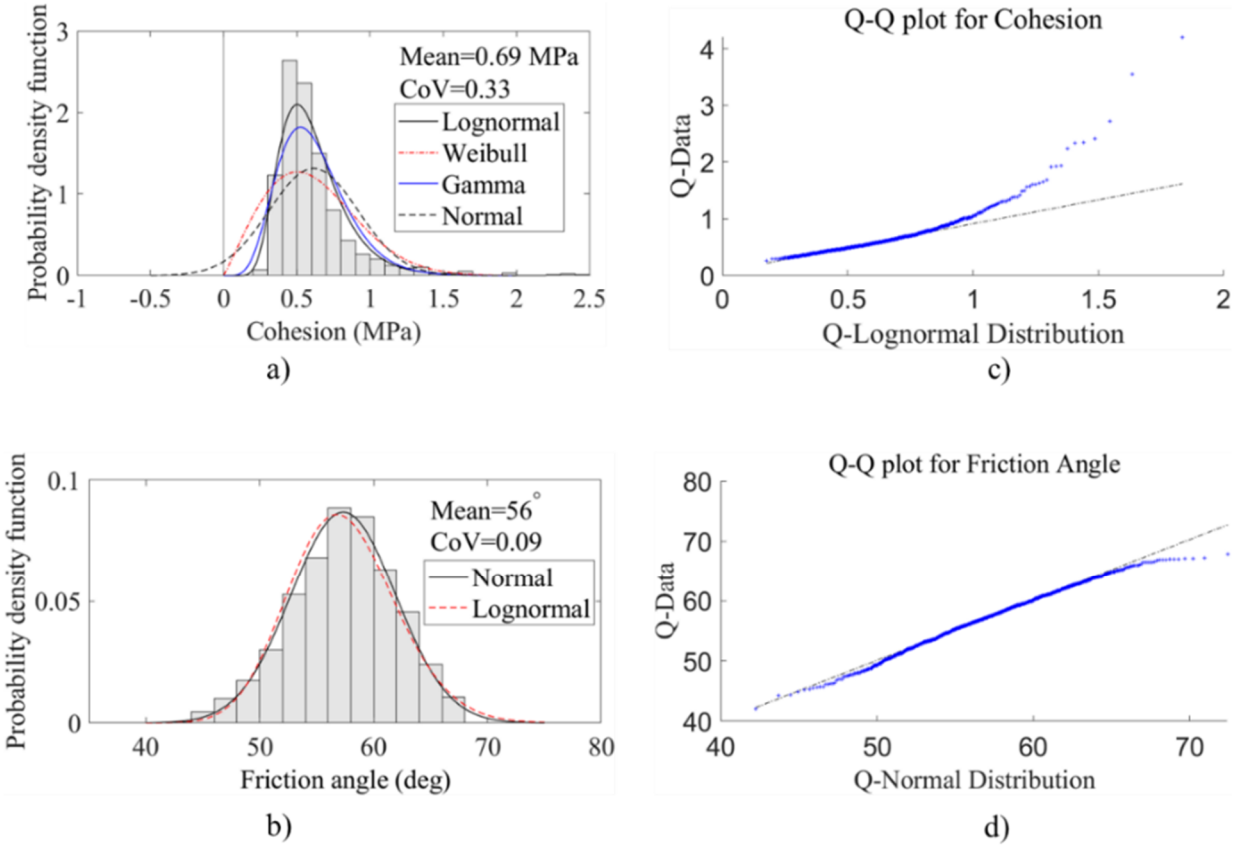

Figure 6 Calculated equivalent Mohr–Coulomb parameters and goodness of fit assumed in scenario 1: (a) PDFs for cohesion; (b) PDFs for friction angle; (c) The Q-Q plot for cohesion; (d) The Q-Q plot for friction angle

The geological structures were examined through stereographic projections aiming to identify possible orientation ranges that could impact slope stability. Figure 7 shows the principal sets identified. The adopted criteria include for analysis all geological structures whose dip direction does not deviate by more than 30° from the slope's dip direction. Given the slope orientation, Set A, which strikes nearly perpendicular, was considered the main large-scale structure that could affect slope stability. This set was further integrated into the probabilistic analysis.

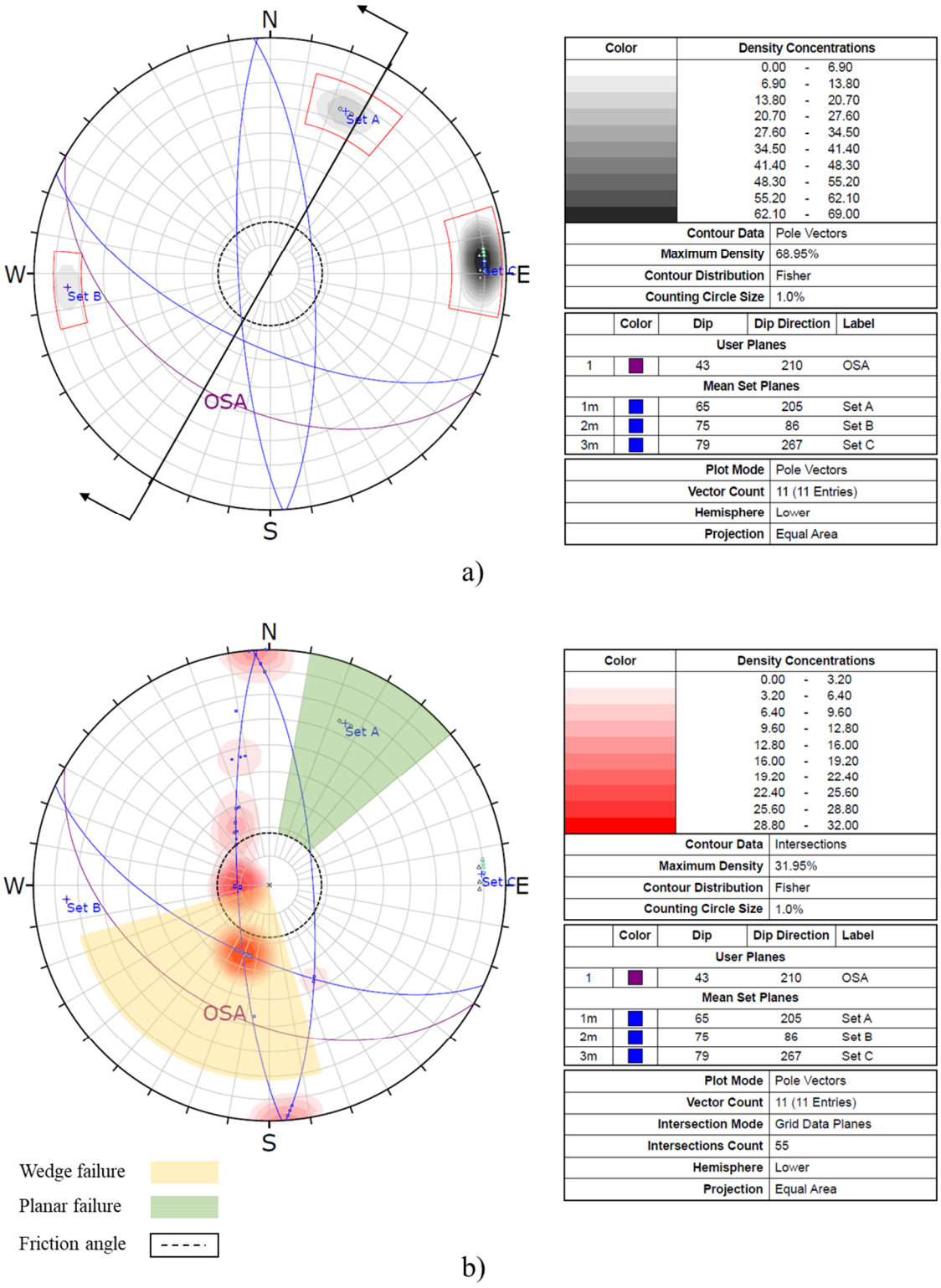

Figure 7 Scenario 1: (a) Main structural orientation of large-scale structures; (b) Structural orientation of planar/wedge-type structures. OSA is the overall slope angle and orientation

Figure 8a shows the calculated FoS and PoF of the isotropic analysis considering a rock mass strength failure mechanism. The mean value of FoS (2.62) can be considered relatively high, while the PoF is very small. Figure 8b shows the calculated FoS and PoF of the anisotropic analysis considering a structurally controlled failure mechanism. The mean FoS (2.21) is approximately 16% lower than the isotropic analysis, although the variation of PoF is negligible in both analyses. From these results, the slope configuration can be deemed

over-conservative. However, this generic slope configuration should only be considered as a preliminary geometry for future analysis.

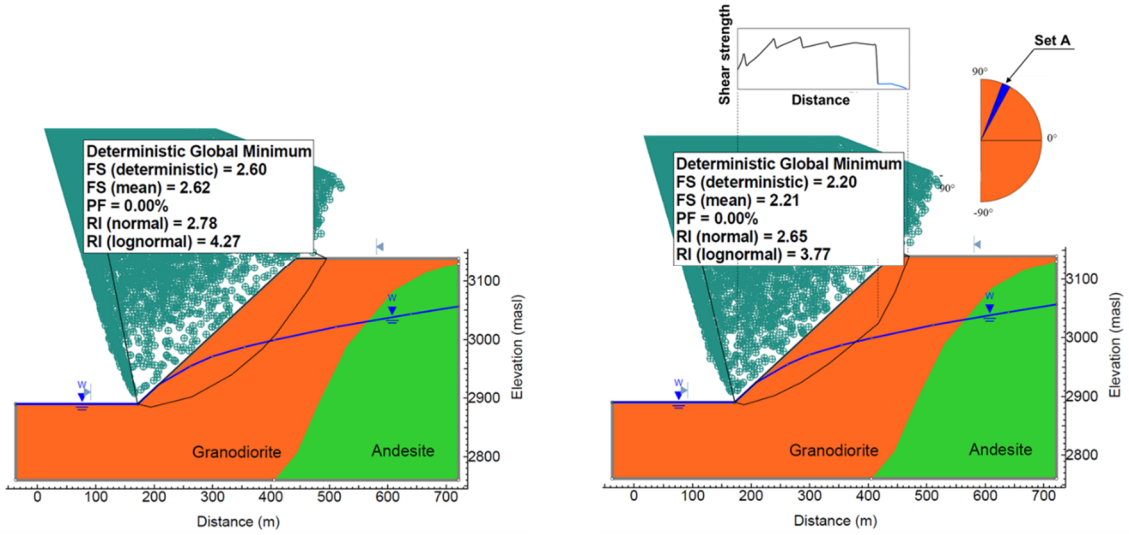

(a) (b)

Figure 8 Limit equilibrium analysis results for (a) Rock mass strength failure; (b) Structurally controlled failure, scenario 1

The results from the Monte Carlo simulation for the isotropic analysis follow a lognormal distribution, as shown in Figure 9a. Figure 9b shows the Q-Q plot to test the goodness of fit. The Kolmogorov–Smirnov test results for lognormal distribution (test statistics 0.03 and a p-value of 0.52) suggest that the observed data adequately follow a lognormal distribution.

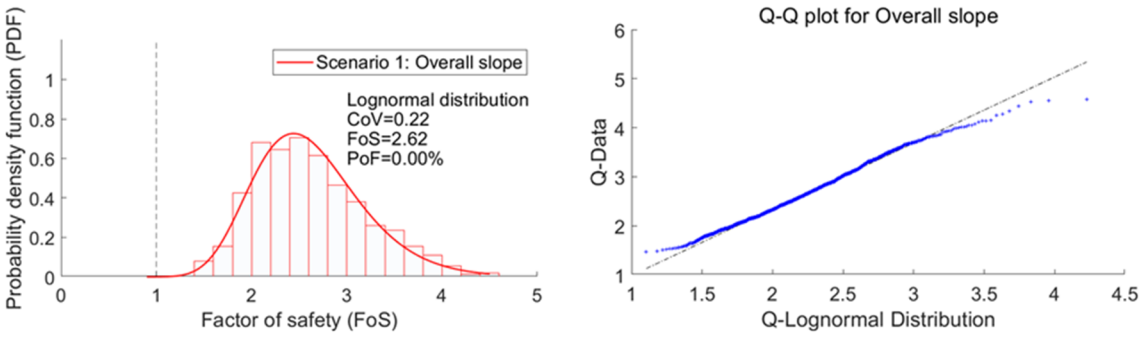

(a) (b)

Figure 9 (a) Calculated distribution of FoS for scenario 1 considering failure through the rock mass; (b) The Q-Q plot of the lognormal distribution fit

The results from the Monte Carlo simulation for the second analysis are shown in Figure 10a, where the PDF follow a lognormal distribution. Figure 10b shows the Q-Q plot to test the goodness of fit. The Kolmogorov–Smirnov test results for lognormal distribution (test statistics 0.02 and a p-value of 0.68) suggest that the observed data adequately follow a lognormal distribution. The lognormal distribution and the calculated COV in both analyses are consistent with the PDF and values assumed for moderate design reliability by Macciotta et al. (2020).

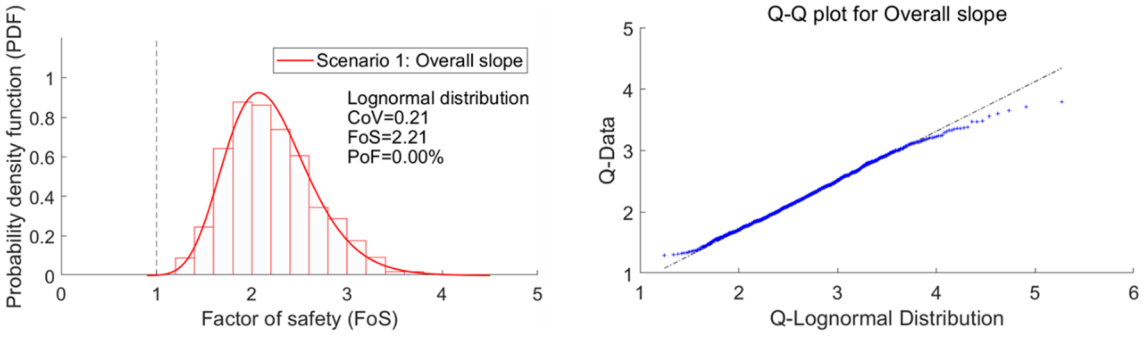

(a) (b)

Figure 10 (a) Calculated distribution of Factor of Safety for scenario 1 considering structurally controlled failure; (b) The Q-Q plot of the lognormal distribution fit

4.2 Second scenario: increased design reliability

This scenario represents a implemented phase slope configuration. The overall slope angle of the slope configuration is 36° at a slope height of 255 m. The COV for the UCS and m_i were obtained based on site-specific data. The COV of UCS for the major lithological units (granodiorite and andesite) was 0.4. The COV of the m_i of 0.20 was adopted for both lithological units. The COV for the GSI of the site was 0.16 and 0.10 for the granodiorite and andesite. The PDF selected was lognormal distribution for UCS and m_i, and a normal distribution for GSI. The dependence between variables was built assuming the same Pearson correlation coefficient obtained previously.

Figure 11 shows the resultant equivalent Mohr–Coulomb parameters and the Q-Q plots for the fitted distributions for the granodiorite rock unit. The Kolmogorov–Smirnov test results for equivalent cohesion following a lognormal distribution (test statistics 0.03 and a p-value 0.28) and for equivalent friction angle following a normal distribution (test statistics 0.03 and a p-value 0.26) suggest close agreement between the observed data and the fitted distribution.

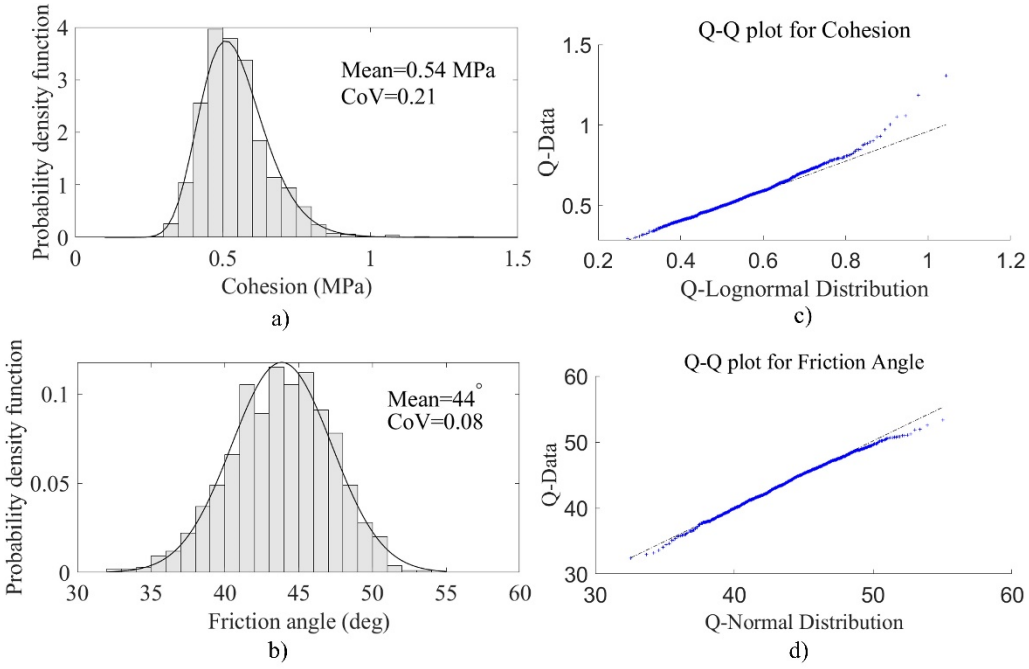

Figure 11 PDFs of equivalent Mohr–Coulomb parameters for the granodiorite unit assumed in scenario 2: (a) Cohesion; (b) Friction angle. The Q-Q plots for: (c) Cohesion; (d) Friction angle

Figure 12 shows the resultant equivalent Mohr–Coulomb parameters and the Q-Q plots for the fitted distributions for the andesite rock unit. The Kolmogorov–Smirnov test results for equivalent cohesion following a lognormal distribution (test statistics 0.03 and a p-value 0.21) and for equivalent friction angle following a normal distribution (test statistics 0.02 and a p-value 0.88) suggest close agreement between the observed data and the fitted distribution.

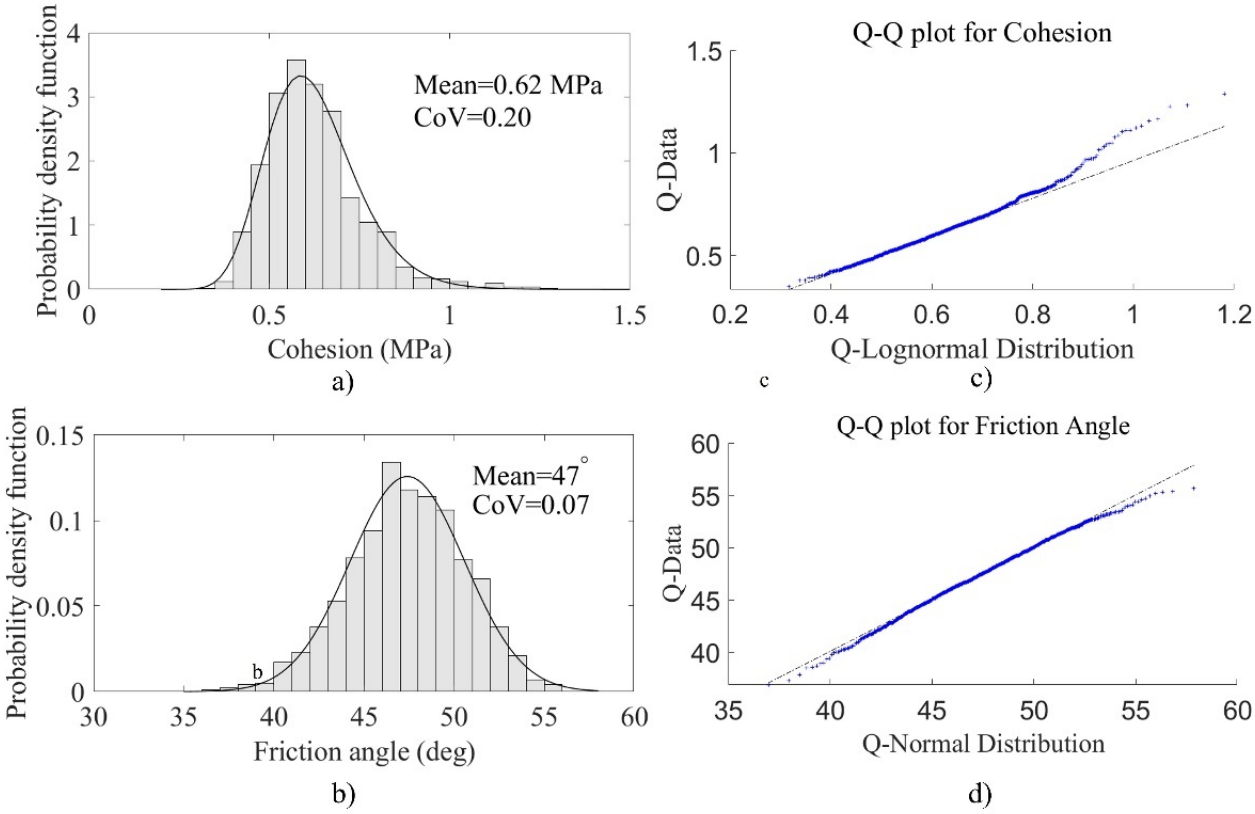

Figure 12 PDFs of equivalent Mohr–Coulomb parameters for the andesite unit assumed in scenario 2: (a) Cohesion; (b) Friction angle. The Q-Q plots: c) Cohesion; (d) Friction angle

Figure 13 shows the stereographic projection of the large-scale structures and orientation of the slope. Four main structural sets are identified. One set has been identified to be adversely oriented. Set E is a non-daylighting planar structure, and the non-daylighting wedge formed in combination with Set G can contribute to developing multi-bench instability.

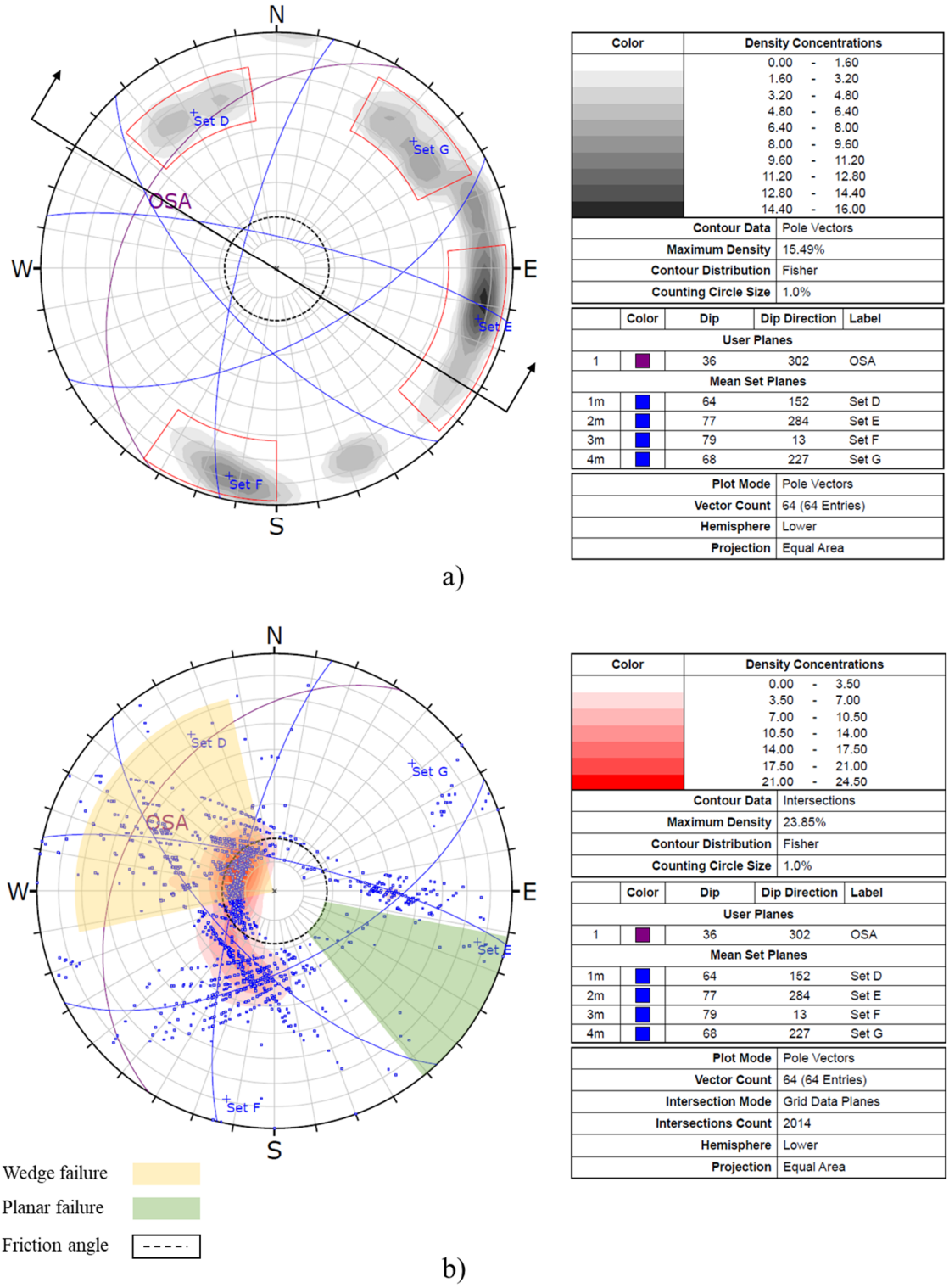

Figure 13 Scenario 2: (a) Main structural orientation of large-scale structures; (b) Structural orientation of planar/wedge-type structures

Figure 14a shows the calculated FoS–PoF for the upper, lower inter-ramp and overall slopes. The failure surfaces for the three slopes are non-circular and shear through the rock mass. The obtained FoS–PoF suggest a stable configuration but with high values of FoS, mainly in the upper inter-ramp slope. Further integration of large-scale structures into the analysis results in lower FoS–PoF (see Figure 14b). However, the PoF in both cases is negligible.

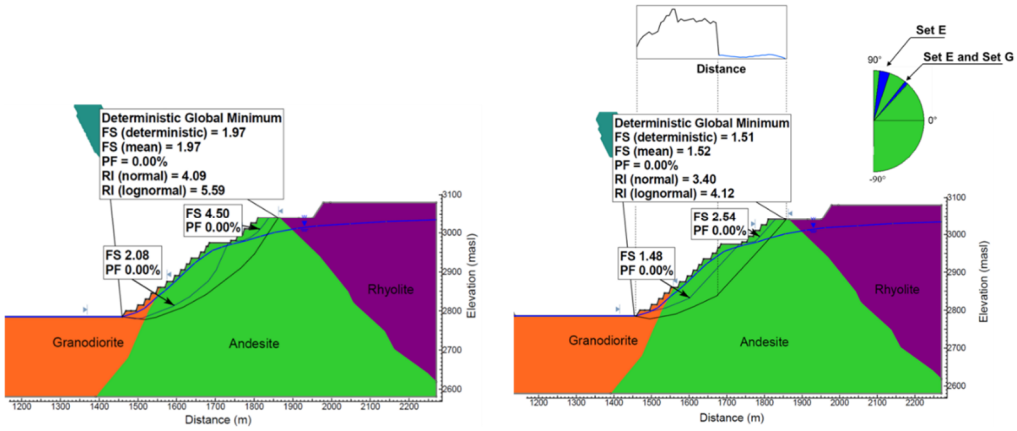

(a) (b)

Figure 14 Limit equilibrium analysis result for: (a) Rock mass strength failure; (b) Structurally controlled failure, scenario 2

The results from the Monte Carlo simulation are shown in Figure 15. The Q-Q plot for each PDF plotted in Figure 15 suggest that lognormal distribution represents the observed data. The Kolmogorov–Smirnov test results of the Overall slope (test statistics 0.03 and a p-value 0.57), lower inter-ramp slope (test statistics 0.03 and a p-value 0.56), and upper inter-ramp slope (test statistics 0.02 and a p-value 0.85) suggest a consistency to the lognormal distribution. The calculated COV_{FoS} is 0.12 for the overall slope and 0.16 for the upper inter-ramp slope.

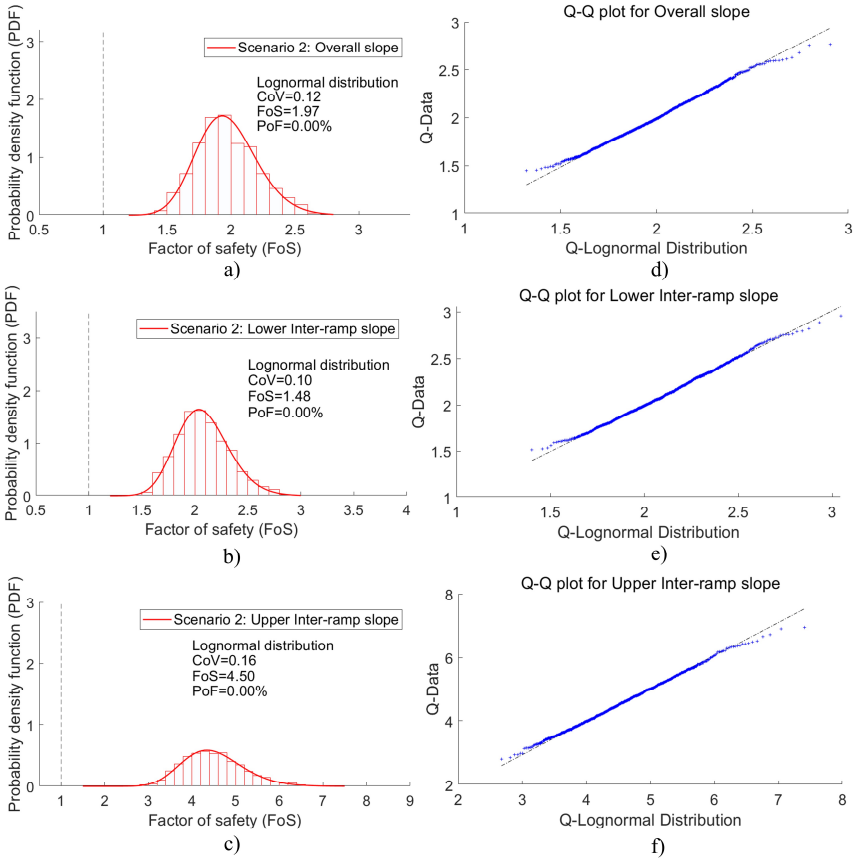

Figure 15 Calculated distribution of FoS for scenario 2 considering rock mass strength failure for (a) Overall slope; (b) Lower inter-ramp slope; (c) Upper inter-ramp slope. The Q-Q plot of the distribution fitted for each Monte Carlo simulation: (d) Overall slope; (e) Lower inter-ramp slope; (f) Upper inter-ramp slope

Figure 16 shows the results from the Monte Carlo simulation. The Q-Q plot for each PDF plotted in Figure 16 suggests that lognormal distribution represents the observed data. The Kolmogorov–Smirnov test results of the overall slope (test statistics 0.02 and a p-value 0.69), lower inter-ramp slope (test statistics 0.03 and a p-value 0.53) and upper inter-ramp slope (test statistics 0.03 and a p-value 0.51) suggest a consistency to the lognormal distribution. The calculated COV_{FoS} is 0.10 for the overall and lower inter-ramp slopes, and 0.13 for the upper inter-ramp slope. The lognormal distribution and the calculated COV_{FoS} in both analyses are consistent with the PDF and values assumed for high design reliability in Macciotta et al. (2020).

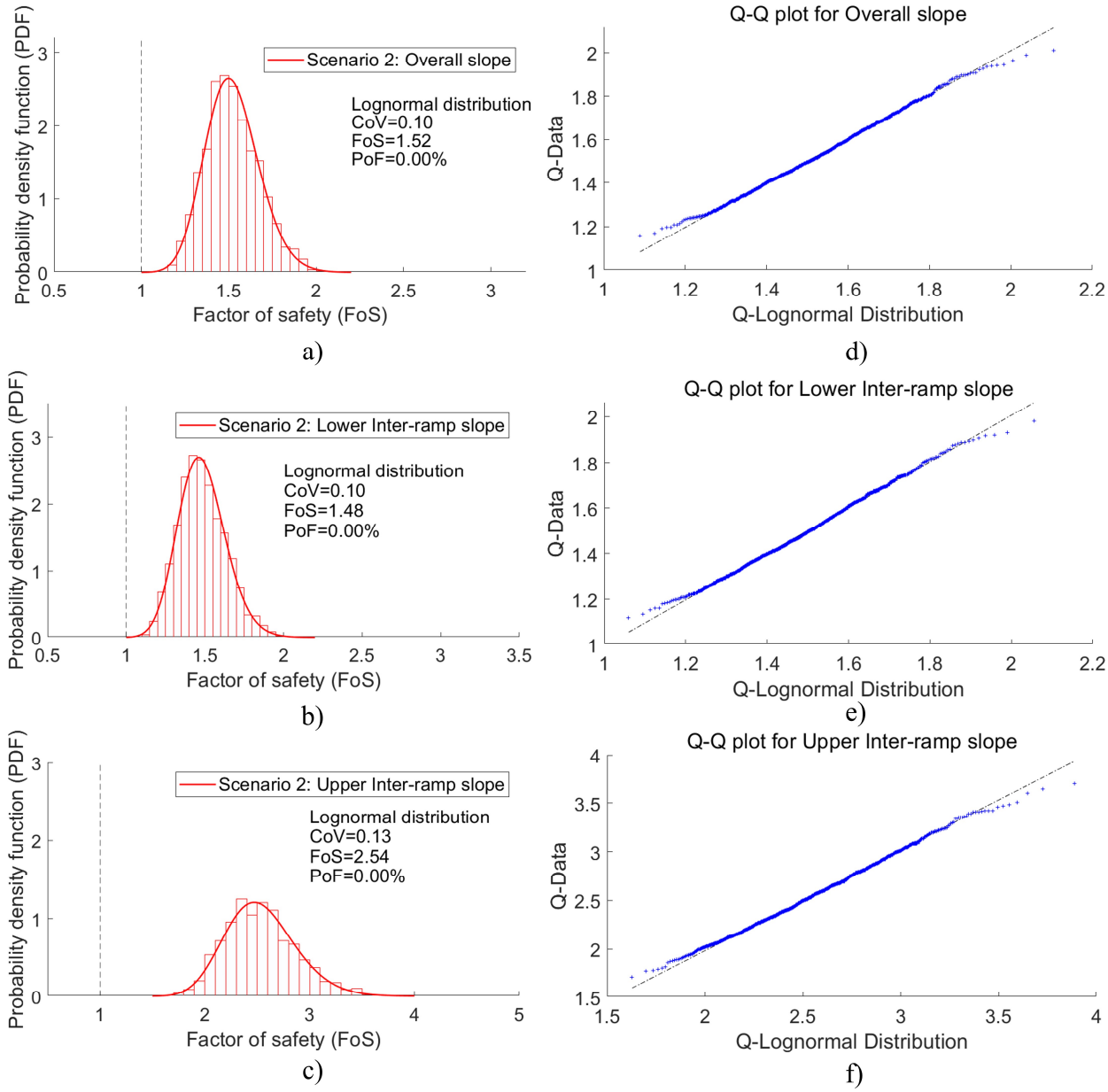

Figure 16 A calculated FoS distribution for scenario 2 considering structurally controlled failure for (a) Overall slope; (b) Lower inter-ramp slope; (c) Upper inter-ramp slope. The Q-Q plot of the distribution fitted for each PDF: (d) Overall slope; (e) Lower inter-ramp slope; (f) Upper inter-ramp slope

4.3 Third scenario: very high design reliability at a mature phase of operations

This scenario represents a mature phase slope design where the lithological units are subdivided in more detail. The rock mass strength parameters are expressed in terms of equivalent cohesion and friction angle. The PDF adopted was normal distribution. The COV was assumed in this scenario as no exact values were reported. Therefore, a COV of less than 0.15 was chosen for equivalent cohesion and a COV of less than 0.10

for an equivalent friction angle was chosen. Table 1 summarises the rock mass strength parameters (Hustrulid et al. 2001).

Table 1 Calibrated rock mass strength properties assumed in scenario 3

Rock unit	Mohr–Coulomb parameters			
	Cohesion (kPa)		Friction angle (deg)	
	Mean	COV	Mean	COV
Altered granodiorite	40	<0.15	25	<0.10
Moderate granodiorite	150	<0.15	28	<0.10
Silificated granodiorite	780	<0.15	36	<0.10
Andesite	150	<0.15	31	<0.10

The structural information of the slope sector is plotted in Figure 17. Four sets are identified. The kinematic evaluation indicates that Set H is a subparallel structure that governs the stability of the slope.

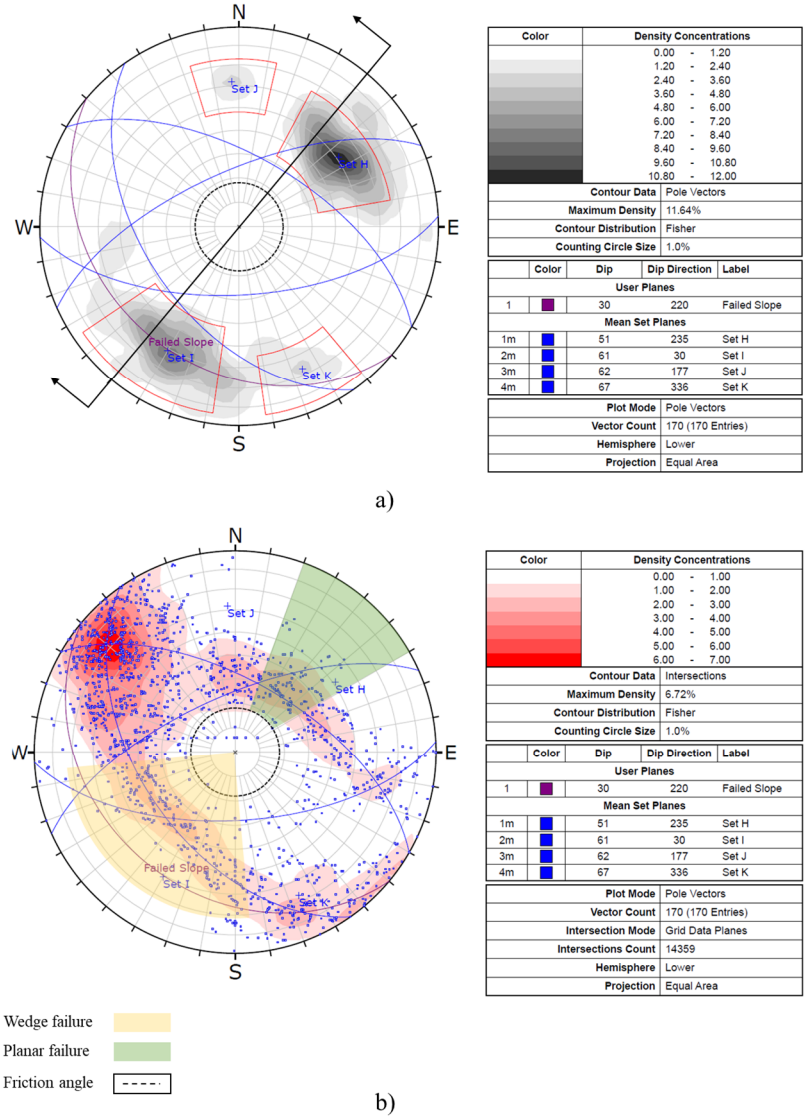

Figure 17 Scenario 3: (a) Main structural orientation of large-scale structures; (b) Structural orientation of planar/wedge-type structures

The Set H was incorporated in the limit equilibrium analysis through generalised anisotropic strength. Figure 18a shows the critical failure surface and the attributed influence of the large-scale structure. The calculated mean FoS is 0.98, with a PoF of 63.3%. Another approach that includes large-scale structures explicitly was also considered. Results from this approach are shown in Figure 18b. The calculated mean FoS is 1.01, and PoF of 42.40%.

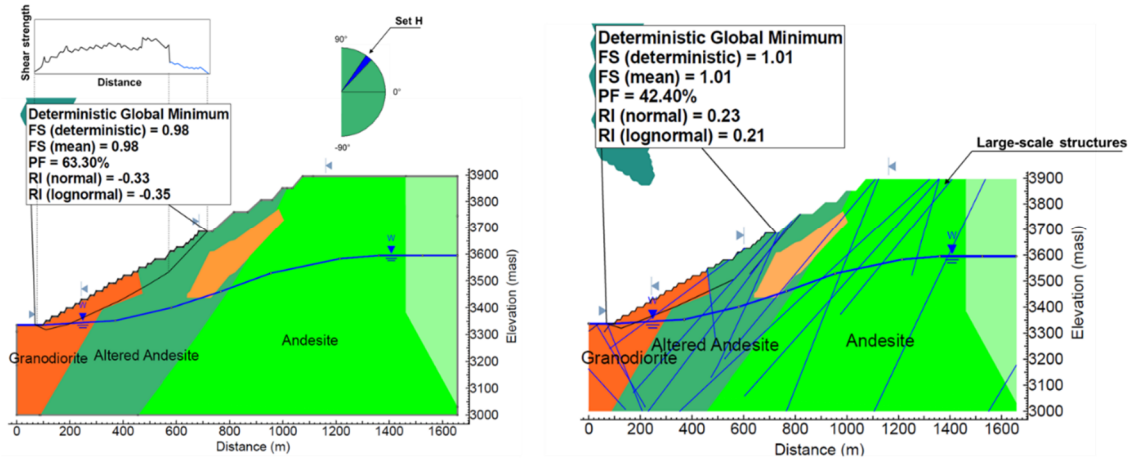

(a) (b)

Figure 18 Limit equilibrium results of back-analysis considering the large-scale structures: (a) Implicitly; (b) Explicitly, scenario 3

Both approaches illustrate similar failure paths, although the implicit approach is sensitive to the extension and continuity of the structures. The results from the Monte Carlo simulation and Q-Q plot for the implicit approach are shown in Figure 19. The calculated COV is 0.05, and the goodness of fit using a Q-Q plot of Kolmogorov–Smirnov test results (test statistics 0.03 and a p-value 0.50) suggests that normal distribution adequately fits the observed data.

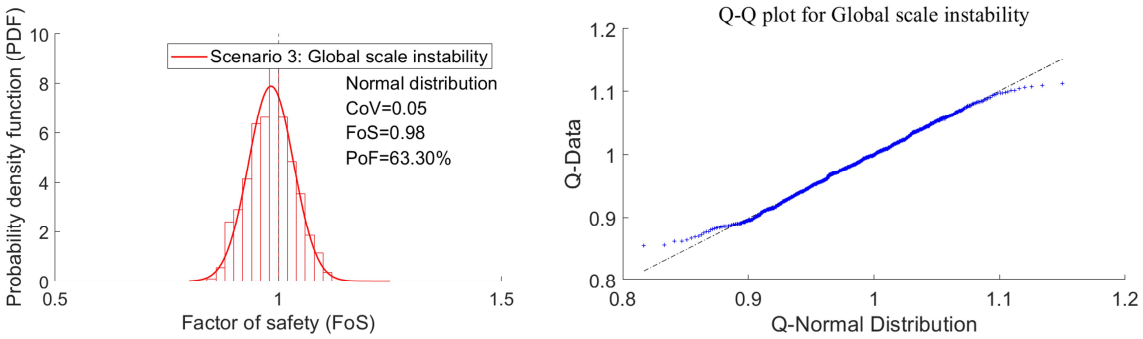

(a) (b)

Figure 19 (a) Calculated distribution of FoS for scenario 3 considering large-scale structures implicitly; (b) The Q-Q plot of the distribution fitted

Similarly, the results of the Monte Carlo simulation and the Q-Q plot for the explicit approach are shown in Figure 20. The calculated COV remains the same as in the previous analysis. The Q-Q plot, along with the Kolmogorov–Smirnov test results (test statistics 0.03 and a p-value 0.53), suggest the observed data follow a normal distribution.

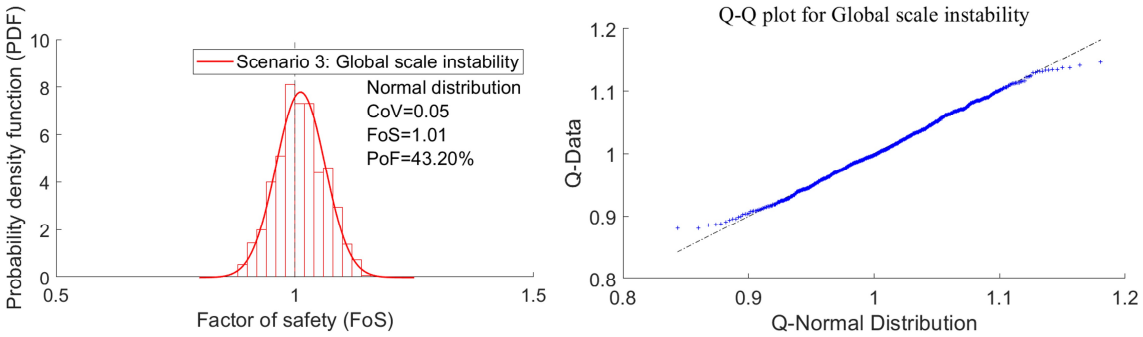

(a) (b)

Figure 20 (a) Calculated distribution of FoS for scenario 3 considering large-scale structures explicitly; (b) The Q-Q plot of the distribution fitted

4.4 Reliability-based DAC

Throughout the scenarios analysed it has been observed that as site-specific data is incorporated, there is a notable reduction in both natural variability and epistemic uncertainty (see Figure 21). This reduction in uncertainty enhances the reliability level of the design as defined by the calculated COV_{FoS}. Moreover, the integration of large-scale structures on probabilistic slope stability analysis increases reliability as it provides defined critical failure paths.

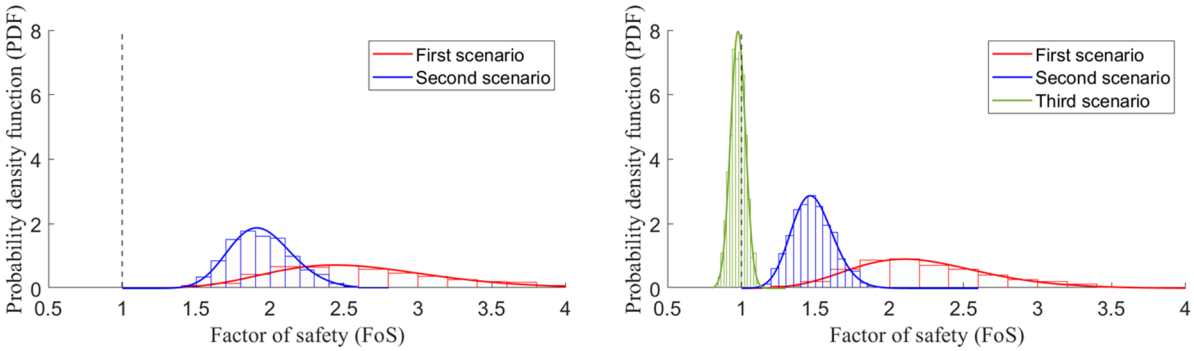

(a) (b)

Figure 21 (a) PDFs for overall scale of rock mass strength failure; (b) PDFs for the overall slope of structurally controlled failure

The calculated pairs of FoS–PoF and associated COV_{FoS} are summarised in Table 2.

Table 2 Summary of FoS–PoF pairs and COV_{FoS} obtained from the three scenarios evaluated

Scenario	Slope design	Slope height (m)	Slope angle (deg)	Analysis	Factor of Safety (FoS)	Probability of failure (PoF)	COV_{FoS}
1	Overall slope	250	43	Isotropic	2.62	0.00	0.22
				Anisotropic (implicit)	2.21	0.00	0.21
2	Overall slope	255	36	Isotropic	1.97	0.00	0.12
				Anisotropic (implicit)	1.52	0.00	0.10
	Upper inter-ramp slope	66	41	Isotropic	4.50	0.00	0.16
				Anisotropic (implicit)	2.54	0.00	0.13
	Lower inter-ramp slope	189	41	Isotropic	2.08	0.00	0.12
				Anisotropic	1.48	0.00	0.10
3	Overall slope	560	30	Anisotropic (implicit)	0.98	67.40	0.05
				Anisotropic (explicit)	1.01	43.20	0.05

Figure 22 shows the results from Table 2 plotted on the 2020 RBDAC. The values enclosed by parenthesis within the matrix represent a mean value following a normal distribution, and the other values represent a mean value following a lognormal distribution. The calculated pairs of FoS–PoF and COV_{FoS} obtained from scenarios 1 and 2 would correspond to ranges defined for a very high level of economic consequence. Scenario 3 is a case of unsuccessful performance of an implemented slope design. Results showed that the scenario did not meet the 2020 RBDAC.

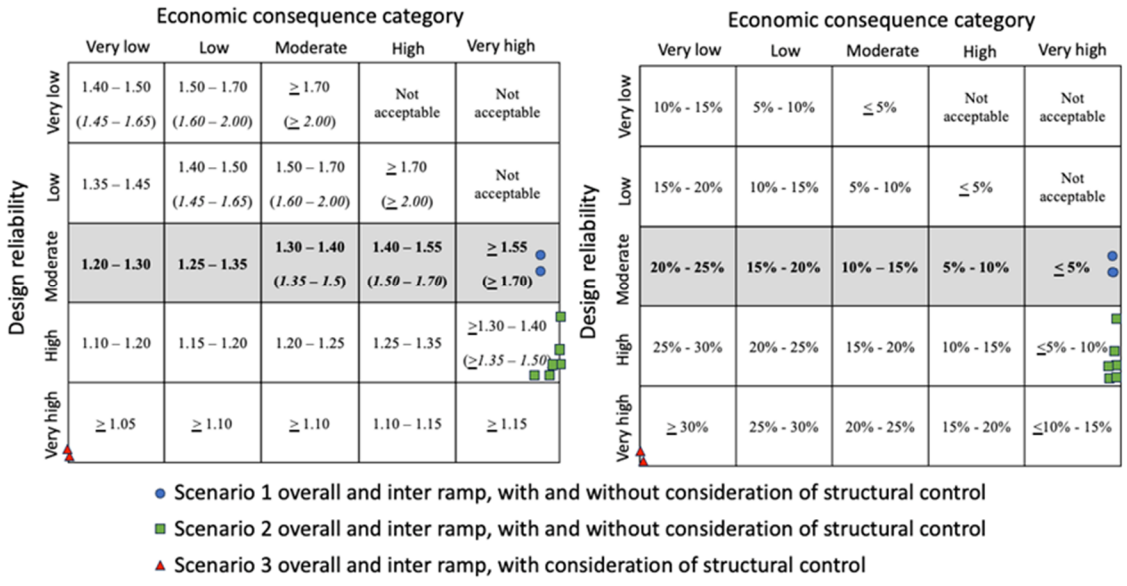

Figure 22 Plot of COV_{FoS}–FoS (left) and COV_{FoS}–PoF (rigth) results in the 2020 RBDAC

These results highlight the importance of understanding uncertainties and the associated reliability so as to improve the risk-informed design process.

4.5 Use of the RBDAC for design

Based on the results from scenario 3, the higher reliability gained can be leveraged to develop a pushback balancing risk and reward. Incorporating large-scale structures into stability analysis highlights the role of uncertainty of the structural model in the FoS–PoF outcomes. Moving forward to the next phase, a slope design should be developed, leveraging the achieved level of reliability in the geotechnical components. In this regard, to determine an optimum configuration, the level of detailed engineering gained from scenario 3 was used as a basis for evaluating potential slope configurations. The slope configuration was assessed with a focus on maintaining adequate safety levels and achieving business rewards. A slope configuration was first evaluated targeting the 2020 RBDAC. The design is interpreted to be associated with a high to very high economic consequence, targeting a minimum FoS of 1.2 and a maximum PoF of 10%, according to the 2020 RBDAC. The slope stability analysis for the suggested slope configuration considered for the next pushback is shown in Figure 23. The design considers mitigative adjustments such as slope flattening and the unloading of about six benches.

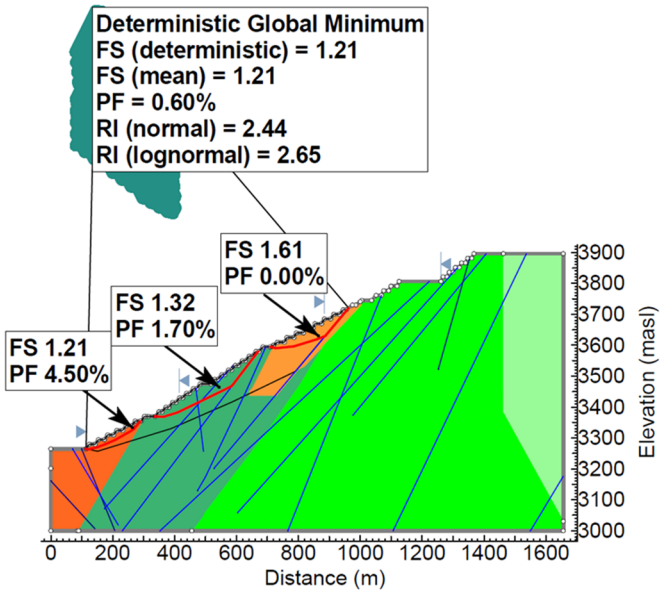

Figure 23 Limit equilibrium analysis results for the next pushback targeting the 2020 RBDAC

The analysis results in Figure 23 suggest a more conservative inter-ramp slope and a reduction in 1° of the overall slope angle to meet the target 2020 RBDAC. Table 3 summarises the calculated pairs of FoS–PoF and COV_{FoS}. The results meet the 2020 RBDAC, and the COV_{FoS} are in line with the range defined in the matrix of the 2020 RBDAC. This design can be considered feasible.

Table 3 Summary of the limit equilibrium analysis for the design proposed for the next pushback

Slope design	Angle (deg)	Height (m)	FoS	PoF (%)	COV_{FoS}
Inter-ramp slope	26	150	1.61	0.0	0.09
	34	225	1.32	1.7	0.11
	26	210	1.21	4.5	0.10
Overall slope	29	540	1.22	0.6	0.07

Conversely, designing with the 2009 DAC that suggests a minimum FoS of 1.3 for overall scale could increase the stripping cost, thus reducing the business reward. To this end, a slope configuration was developed to meet the 2009 DAC. Figure 24 shows the limit equilibrium analysis targeting the 2009 DAC. The analysis results in Figure 24 suggest that OSA should be decreased by 1° compared to the design targeting the 2020 RBDAC. Additionally, the slope design targeting the 2009 DAC will result in mining an additional 30.61 Mt

considering a total pit sector length of 500 m affected by this design. The volume calculated is an estimate, however, three-dimensional analysis can provide more precise values.

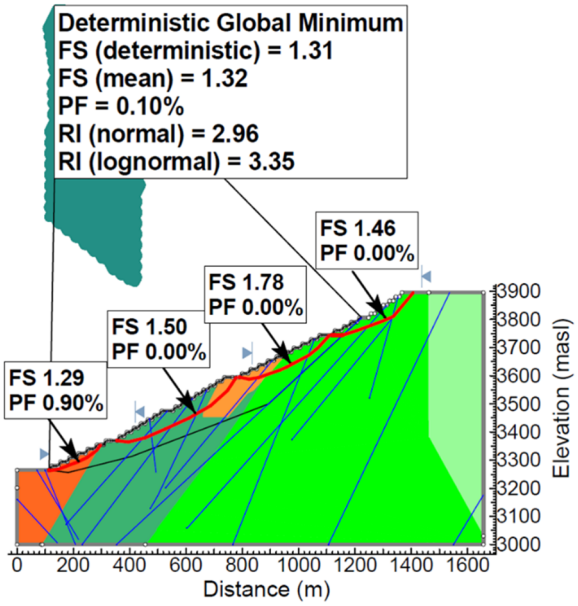

Figure 24 Limit equilibrium analysis results for the next pushback targeting the 2009 DAC

Figure 25 shows a comparison between the slope design targeting the 2009 DAC and 2020 RBDAC. The comparison shown in this figure provides insights into potential trade-offs between safety, excavation volume and economic benefits by adopting the 2020 RBDAC.

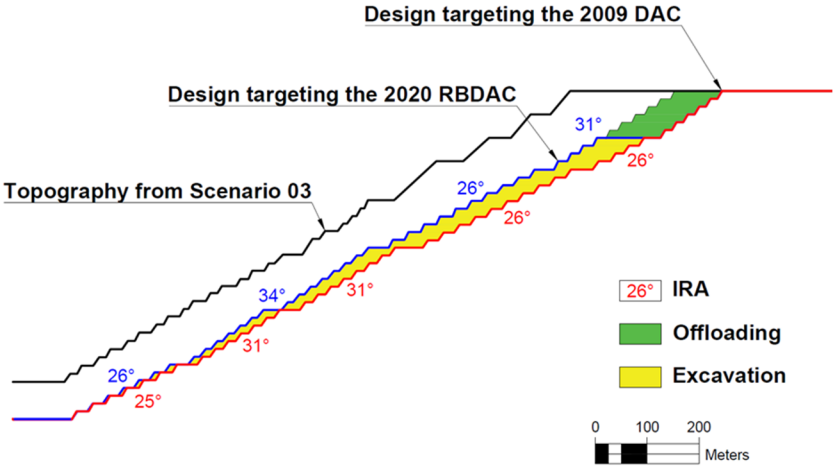

Figure 25 Slope design configurations for the next pushback targeting both the 2020 RBDAC and the 2009 DAC

5 Conclusion

The flexibility and the applicability of an RBDAC in the slope design are demonstrated in this paper. A parametric study was adopted to assess the influence of uncertainties in the slope design process through probabilistic slope stability analyses. Three scenarios have been evaluated considering different levels of engineering effort. Throughout the scenarios analysed, it has been observed that as specific data such as rock mass properties and geological structures are incorporated, the uncertainty is reduced, thus increasing the reliability of the slope design.

The methodology adopted in this study follows the state of practice in the design of open pit slopes. The COV has been adopted in this study as a measure of uncertainty. The input parameters for the rock mass

parameters have been evaluated through adequate probabilistic density functions. Moreover, the geological structures have been evaluated through stereographic projections. It has been observed that integration of geological structures in the stability analysis leads to a reduction in the COV of the FoS distribution. The results of the first scenario show moderate reliability for a very high consequence category, while the second scenario demonstrates high reliability. The third scenario incorporates a back-analysis of a mature slope configuration and shows high reliability.

A comparison between the RBDAC matrix and the 2009 DAC has been conducted for a pushback design. The RBDAC matrix results in a 1° difference in the overall slope angle and requires a lower mining volume compared to the 2009 DAC. The study demonstrates the practicality and flexibility of the RBDAC matrix and highlights the potential optimisation gains by considering increased knowledge of slope performance and design reliability. Evaluating design reliability based on specific engineering efforts and risk assessment is essential for slope design optimisation.

Acknowledgement

The authors acknowledge the financial support of the LOP project that allowed the development of this paper.

Reference

Baecher, GB & Christian, JT 2003, *Reliability and Statistics in Geotechnical Engineering*, John Wiley & Sons, New York, pp. 19–33.

Bedi, A & Harrison, JP 2013, 'Characterisation and propagation of epistemic uncertainty in rock engineering: a slope stability example', *Proceedings of the ISRM International Symposium - EUROCK 2013*, International Society for Rock Mechanics, Lisbon.

Bewick, RP, Amann, F, Kaiser, PK & Martin, CD 2015, 'Interpretation of UCS test results for engineering design', *Proceedings of the 13th ISRM International Congress of Rock Mechanics*, International Society for Rock Mechanics, Lisbon.

Creighton, A, Bixley, M, Elmouttie, M, Hassall, M, Macciotta, R & Juldz, A 2022, 'A reliability-based design acceptance criteria approach for inter-ramp and overall open pit slopes', Proceedings of the *International Slope Stability 2022 Symposium*, Tucson.

Darling, P 2011, 'Introduction to open-pit mining', *SME Mining Engineering Handbook*, 3rd edn, Society for Mining, Metallurgy & Exploration, Engelwood.

Ferson, S & Ginzburg, LR 1996, 'Different methods are needed to propagate ignorance and variability', *Reliability Engineering & System Safety*, vol. 54, no. 2-3, pp. 133–144, https://doi.org/10.1016/S0951-8320(96)00071-3

Gaida, M, Cambio, D, Robotham, ME & Pere, V 2021, 'Development and application of a reliability-based approach to slope design acceptance criteria at Bingham Canyon Mine', in PM Dight (ed.), *SSIM 2021: Second International Slope Stability in Mining*, Australian Centre for Geomechanics, Perth, pp. 83–94, https://doi.org/10.36487/ACG_repo/2135_02

Hadjigeorgiou, J & Harrison, JP 2011, 'Uncertainty and sources of error in rock engineering', *Proceedings of the 12th ISRM Congress*, International Society for Rock Mechanics, Lisbon.

Hoek, E 1998, 'Reliability of Hoek-Brown estimates of rock mass properties and their impact on design', *International Journal of Rock Mechanics and Mining Sciences*, vol. 53, no. 1, pp. 63–68, https://doi.org/10.1016/S0148-9062(97)00314-8

Hoek, E & Bray, J 1981, *Rock Slope Engineering*, 3rd edn, Institution of Mining and Metallurgy, London.

Hoek, E, Carranza-Torres, C & Corkum, B 2002, 'Hoek-Brown criterion – 2002 edition', in R Hammah, W Bawden, J Curran & M Telesnicki (eds), *Proceedings of the 5th North American Rock Mechanics Symposium and 17th Tunnelling Association of Canada Conference,* University of Toronto, Toronto., pp. 267–273.

Hoek, E & Brown, ET 2018, 'The Hoek–Brown failure criterion and GSI – 2018 edition', *Journal of Rock Mechanics and Geotechnical Engineering*, vol. 11, no. 3, pp. 445–463, https://doi.org/10.1016/j.jrmge.2018.08.001

Hudson, JA & Feng, X 2015, 'Uncertainty and risk', *Rock Engineering Risk*, CRC Press/Balkema, Leiden, pp. 9–27.

Hustrulid, WA, McCarter, MK & Van Zyl, DJA 2001, 'Slope stability at Escondida mine', in *Slope Stability in Surface Mining*, Society for Mining, Metallurgy & Exploration, Engelwood, pp. 153–162.

Kiureghian, AD & Ditlevsen, O 2008, 'Aleatory or epistemic? Does it matter?', *Structural Safety*, vol. 31, no. 2, pp. 105–112, https://doi.org/10.1016/j.strusafe.2008.06.020

Ma, T, Cami, B, Javankhoshdel, S, Yacoub, T, Corkum, B & Curran, J 2022, 'Effect of disturbance factor distribution function on stability of an open pit mine', *Proceedings of the 56th U.S. Rock Mechanics/Geomechanics Symposium*, American Rock Mechanics Association, Alexandria, https://doi.org/10.56952/ARMA-2022-2221

Martin, D & Stacey, P 2018, *Guidelines for Open Pit Slope Design in Weak Rocks*, CSIRO Publishing, Clayton South.

Macciotta, R, Creighton, A & Martin, CD 2020, 'Design acceptance criteria for operating open pit slopes: an update', *CIM Journal,* vol. 11, no. 4, pp. 248–265, https://doi.org/10.1080/19236026.2020.1826830

Macciotta, R, Creighton, A & Martin, CD 2021, 'Design acceptance criteria and risk tolerance for inter-ramp and overall open pit slopes', *Canadian Geotechnique*, vol. 2, no. 3, pp. 48–51.

Macciotta, R, Creighton, A & Martin, CD 2022, 'Reliability based design acceptance criteria for inter-ramp and overall pit slopes – fundamental considerations and mathematical background', *Proceedings of the International Slope Stability 2022 Symposium*, Tucson.

Padilla, RA, Titley, SR & Pimentel, F 2001, 'Geology of the Escondida porphyry copper deposit, Antofagasta Region, Chile', *Economic Geology*, vol. 96, no. 2, pp. 307–324, https://doi.org/10.2113/gsecongeo.96.2.307

Phoon, KK & Ching, J 2015, *Risk and Reliability in Geotechnical Engineering*, CRC Press, Boca Raton, pp. 3–72.

Phoon, KK & Retief, JV 2016, *Reliability in Geotechnical Structures in ISO2394*, CRC Press/Balkema, Leiden, pp. 49–82.

Rapiman, MM & Sepulveda, MR 2006, 'Slope optimization at Escondida Norte Open Pit', in *Proceedings of Stability of Rock Slopes*, The South African Institute of Mining and Metallurgy Symposium Series, Johannesburg, pp. 265–278.

Rafiei Renani, H & Martin, CD 2020, 'Slope stability analysis using equivalent Mohr–Coulomb and Hoek–Brown criteria', *Rock Mechanics and Rock Engineering*, vol. 53, no. 1, pp. 13–21, https://doi.org/10.1007/s00603-019-01889-3

Rafiei Renani, H, Martin, CD, Varona, P 2019, 'Stability analysis of slopes with spatially variable strength properties.', *Rock Mechanics and Rock Engineering*, vol. 52, no. 10, pp. 3791–3808, https://doi.org/10.1007/s00603-019-01828-2

Read, J & Stacey, P 2009, *Guidelines for Open Pit Slope Design*, CSIRO Publishing, Collingwood.

Rocscience Inc 2022, DIPS-Graphical and statistical analysis of orientation data, computer software, Toronto, Canada.